

Impact of Molecular Symmetry on Single-Molecule Conductance

Emma J. Dell,^{†,§} Brian Capozzi,^{‡,§} Kateri H. DuBay,[†] Timothy C. Berkelbach,[†] Jose Ricardo Moreno,[†] David R. Reichman,[†] Latha Venkataraman,^{*,‡} and Luis M. Campos^{*,†}

[†]Department of Chemistry, Columbia University, New York, New York 10027, United States

[‡]Department of Applied Physics and Mathematics, Columbia University, New York, New York 10027, United States

Supporting Information

ABSTRACT: We have measured the single-molecule conductance of a family of bithiophene derivatives terminated with methyl sulfide gold-binding linkers using a scanning tunneling microscope based break-junction technique. We find a broad distribution in the single-molecule conductance of bithiophene compared with that of a methyl sulfide terminated biphenyl. Using a combination of experiments and calculations, we show that this increased breadth in the conductance distribution is explained by the difference in 5-fold symmetry of thiophene rings as compared to the 6-fold symmetry of benzene rings. The reduced symmetry of thiophene rings results in a restriction on the torsion angle space available to these molecules when bound between two metal electrodes in a junction, causing each molecular junction to sample a different set of conformers in the conductance measurements. In contrast, the rotations of biphenyl are essentially unimpeded by junction binding, allowing each molecular junction to sample similar conformers. This work demonstrates that the conductance of bithiophene displays a strong dependence on the conformational fluctuations accessible within a given junction configuration, and that the symmetry of such small molecules can significantly influence their conductance behaviors.

The drive to miniaturize the active components in electronic devices requires that we understand the transport characteristics of molecular scale circuits.¹ Measurement of the conductance of single metal-molecule-metal junctions has thus become an important characterization tool in the sub-10 nm scale.² In such measurements, it is well-known that the conductance of single molecule junctions is sensitive to several experimental parameters such as the electrode structure, the orientation of the molecule-metal bonds, and the conformation of the molecular backbone.³ The pervasiveness of thiophenes in bulk organic electronic and photonic devices⁴ makes their properties in single molecule devices of particular interest. In comparing the charge transport of a bithiophene derivative with that of a biphenyl derivative, we show here that conductance is also dependent on the degree of symmetry given by the molecular backbone in a metal-molecule-metal junction. Specifically, we find that the difference in ring symmetry, 6-fold for phenyl rings versus 5-fold for thiophene rings, strongly impacts the rotational barrier that the less symmetric bithiophene is subject to when bound between two

electrodes. The rotational barrier for the more symmetric biphenyl is only slightly impacted by the binding event, while that for the less symmetric bithiophene is significantly altered. This difference in rotational barriers is manifested in the difference in conductance distributions measured for the two molecules.

In order to investigate the role of molecular backbone symmetry on the charge transport characteristics measured at the single-molecule level, we first compare the conductance of a bithiophene derivative (T2) terminated with methyl sulfide end groups that bind gold electrodes with the biphenyl analog (Figure 1A).⁵ Thiophene moieties were synthesized by using

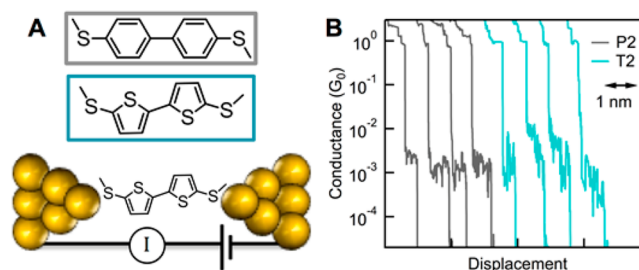


Figure 1. (A) Structure of T2 (blue) and P2 (gray) and a schematic of the scanning tunneling microscope break-junction (STM-BJ) technique. (B) Sample conductance traces measured for P2 and T2 at 90 mV.

both Stille and Suzuki cross-coupling reactions.⁶ The methyl sulfide end groups were introduced through deprotonation with *n*-butyl lithium, followed by a nucleophilic reaction with dimethyl disulfide. The compounds were purified using column chromatography and characterized by ¹H NMR, ¹³C NMR, mass spectrometry, and UV–vis absorption (Supporting Information (SI)). The biphenyl derivative, 4,4'-bis-(methylsulfide)biphenyl (P2), was purchased from Sigma Aldrich and used without purification.

We measured the conductance (current/voltage) of the molecules using a scanning tunneling microscope break-junction (STM-BJ) technique under ambient conditions.^{2a,d} Gold atomic point contacts were repeatedly formed and then broken by driving the gold tip in and out of contact with a gold-on-mica substrate. Individual molecular junctions were formed when the gold point contacts were broken in a solution of the

Received: June 3, 2013

Published: August 1, 2013

target molecule (10 mM concentration, 90 mV bias voltage) in 1,2,4-trichlorobenzene (TCB). Thousands of conductance–displacement traces were collected; each trace displays plateaus close to integer multiples of the quantum of conductance, G_0 ($2e^2/h$), and an additional plateau-like feature at a molecule-specific conductance range (Figure 1B). These additional plateaus indicate that a conducting metal–molecule–metal bridge is formed after the gold point contact is ruptured.

To determine the most frequently measured conductance value for these two molecules, we compile all measured conductance traces into logarithmically binned one-dimensional histograms.⁷ We use logarithmically binned histograms to highlight the conductance peaks as a linear-binned histogram, for **T2** displays a very broad feature which cannot be characterized easily; this excessive breadth is unique to this molecule and can be placed into context by comparing it with the width of the **P2** conductance distribution (Figure 2A and

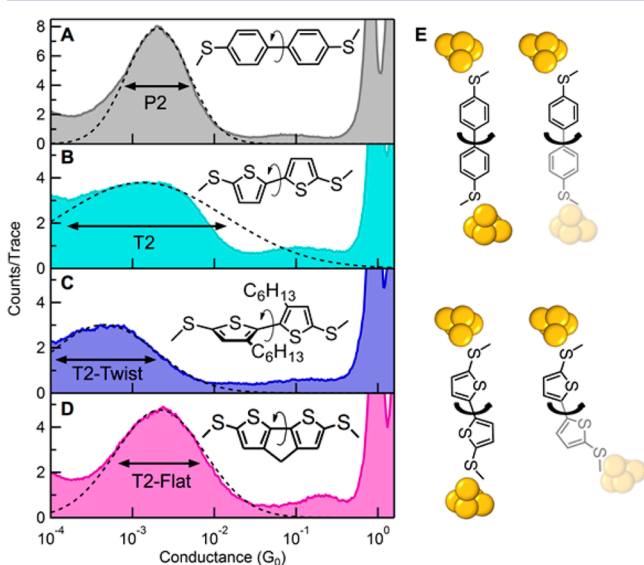


Figure 2. Logarithmically binned conductance histograms of (A) biphenyl (**P2**); (B) bithiophene (**T2**); (C) **T2-twist**; and (D) **T2-flat** showing a Gaussian fit with fwhm indicated by the arrows. (E) Schematic illustrating how ring symmetry impacts rotations for **P2** and **T2** when bound in a junction.

2B). For measurements with the STM-BJ technique where thousands of junction structures are sampled to determine the most frequently observed conductance values, the width in the distribution reflects variations in conductances due to variations in molecular junction structure. Junction structure includes the electrode structure, the orientation of the Au–S–C donor–acceptor bonds relative to the molecular backbone,^{3d} and the average dihedral twist angle between the two rings which is constrained by the details of the electrode structure.^{2d} Thus in these two-ring systems, some width to the conductance distribution is expected. What is surprising, however, is that the conductance distribution of **T2** is much greater than that of **P2**, and as both systems include the same electrodes and methyl sulfide binding groups, we surmise that a factor intrinsic to the molecular structure is the cause.

At room temperature, when not bound in any junction, both phenyl rings and thiophene rings are able to freely rotate due to thermal fluctuations. Since the time scales of the rotations are significantly smaller than the time scales of our measurements (100 μ s), we expect that the conductance measurements

represent an average conductance through the various conformers that are energetically accessible in the junction. If these freely rotating conformers are locked when bound in a junction, we would expect to see a difference in conductance distributions. The rotational degrees of freedom for a 6-fold phenyl system are different from that of a 5-fold thiophene system when considering the rotation axis defined by the attachment points of the linker to the Au electrodes. Rotations in biphenyl are almost unaffected by containment in a junction, but for a bithiophene bound in a junction, the barrier to rotation is increased since changing the torsion angle necessitates either moving the gold atom to which the molecule is attached (Figure 2E) or deforming the rest of the structure to accommodate the change. Thus, in single biphenyl junctions, conductance will be independent of the molecule’s conformation, while in bithiophene junctions conductance will be strongly dependent on the molecule’s conformation imposed by its binding geometry. This striking difference yields a conductance distribution for **T2** that spans over 2 orders of magnitude at full width at half max (fwhm), almost twice that of **P2**.

Within this reasoning, junction elongation also plays a crucial role in the measured conductance distributions. From Figure 1B, we see that individual **T2** conductance traces display more variation than the **P2** ones. As the junction is elongated, the molecule generally alters its binding sites on the electrodes, thus each measured trace consists of conductance measurements of different structures.⁸ For **P2**, such changes in geometry would not be expected to impact the measured conductance over the course of a single conductance trace. The molecule’s inter-ring rotations will be unaffected, and the measured conductance over the course of a trace will continue to be an average over all such conformations. This situation is drastically different for **T2**. Since rotations for this molecule are restricted based upon its binding geometry, changes in junction geometry due to elongation will manifest as changes in conductance, as is seen in the sample traces shown in Figure 1.

In order to experimentally investigate the relation between conductance and allowed rotations in **T2**, we synthesized two other bithiophene derivatives (Figure 2C and 2D): **T2-flat**, where the internal rotation between the aromatic rings is locked by a saturated linker, and **T2-twist**, where hexyl chains at the 3,3’ positions force the molecule into a twisted conformation (synthetic details are given in the SI). These derivatives restrict the rotation around the inter-ring torsion, and therefore represent “frozen snapshots” of the rotation. The 1D logarithmically binned conductance histograms of these two molecules are shown in Figure 2C and 2D. We see that the conductance distributions for both the twisted and planar bithiophene derivatives are considerably narrower than that of **T2**. In addition, the conductance peak of **T2-flat** overlaps the higher-conducting portion of the conductance peak of **T2**, which would be expected from its increased conjugation due to the forced planarity. In contrast, the peak of **T2-twist** overlaps the lower-conducting portion of the **T2** peak; this would also be expected from its reduced conjugation. Furthermore, the conductance distributions for **P2** and **T2-flat** are of similar width, which is to be expected.^{2d} Although **P2** has more rotational freedom, the time scales of the measurement (10 μ s) are large enough that all of the conformational fluctuations are averaged, so a narrow conductance distribution is indeed expected.

To probe the relation between conductance and symmetry, we calculated the torsional potential energy curves for biphenyl and the bithiophene derivatives using OPLS-SB-T, a classical force field that has been specifically designed to correctly represent the effects of conjugation in such biaryl systems.⁹ For each system, the minimum energy unbound structure was determined while restricting the torsional angle, θ , to a value between 0° to 180° in steps of 10° . This resulted in the solid potential energy curves shown in Figure 3A–D. In order to

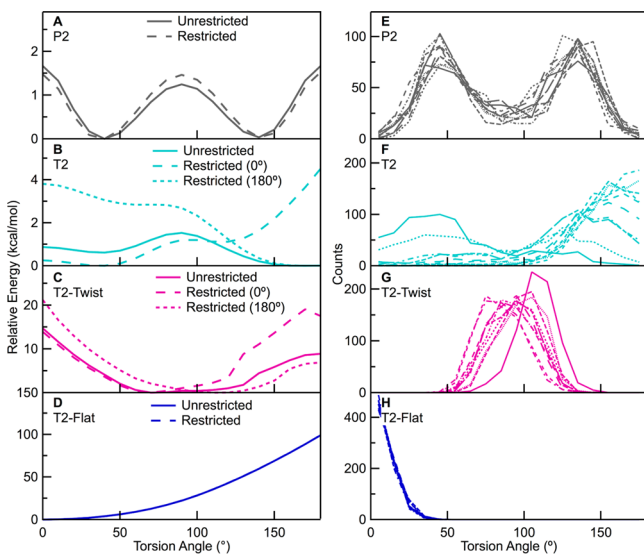


Figure 3. (A–D) Calculated unrestricted (solid) and restricted (dashed) potential energy curves as a function of internal torsion angle. (Note: Only one restricted curve is shown for **P2** and **T2-flat** as detailed in the text.) (E–H) The distributions of torsion angles sampled during the first 10 restricted MD simulations (out of 500), where the distance between their Au-binding sulfur atoms is restricted to its initial value to reproduce the constraints imposed on each molecule when it binds in the break junction. Each curve represents the torsion angle distribution from an individual run.

explore the additional barriers to torsional fluctuations that could be induced upon binding in the junction, the structures were then minimized with an additional restriction on the distance between the two sulfur atoms that act as Au-attachment sites. For **P2** and **T2-flat**, these atoms were frozen in their optimal positions when $\theta = 0^\circ$ (as obtained from the minimized structure in the first step). For **T2** and **T2-twist**, these atoms were frozen in their optimal positions both when $\theta = 0^\circ$ and when $\theta = 180^\circ$. The $\theta = 180^\circ$ case was not investigated for **P2**, as it is identical to the $\theta = 0^\circ$ case, or for **T2-flat** as it is clearly an inaccessible configuration. The potential energy curves calculated in the presence of these additional restrictions are shown in Figure 3A–D as dashed lines.

We see that for **P2** the restricted and unrestricted geometry potential energy curves are quite similar (Figure 3A), suggesting that junction binding should not bias the distribution of inter-ring torsional angles sampled during a conductance measurement. In contrast, the torsional potential of **T2** is significantly modified when the Au-binding S atoms are restricted, as evident in Figure 3B. This is due to the 5-fold symmetry of the thiophene ring, which imposes a constraint as discussed above. Given the heights of the barriers introduced when the distance between the Au-binding S atoms is fixed,

which are several times the expected thermal fluctuations of the system at room temperature, the observed distribution of torsion angles in bithiophene will be significantly biased by the binding orientation of each molecule in the break junction. Since every measurement run has a different electrode structure (and this structure is changed as the junction is elongated), we expect the distributions of bithiophene torsional angles to vary significantly from junction to junction, and possibly also within each junction as it is elongated. As a result, the conductance measurements capture variations in junction binding, widening the measured conductance peak.

To further understand how the trapping of molecules in a junction might slow or restrict inter-ring rotations, we carried out room temperature molecular dynamics (MD) simulations of the four molecules. The details of the calculations are given in the SI, but, briefly, we ran atomistic gas phase simulations within the NVT ensemble using the OPLS-SB-T potential.⁹ In an initial step, all atoms were allowed to move without restriction, as would be the case for the molecules prior to their binding in the junction. Then, in the second step, the distance between the molecules' terminal sulfurs was held fixed in order to simulate the binding event (the pulling forces were not represented in this model). After some equilibration time, the average value of the inter-ring dihedral angle, θ , and the average value of $\cos^2(\theta)$ (which is proportional to the conductance, as shown in SI Figure S2^{2d}) were measured for each run. Repeating this procedure for 500 different "binding" configurations produced significantly broader estimated conductance histograms for bithiophene than biphenyl, confirming that the significant differences in the potential energy curves are manifested in the room temperature dynamics of the different molecules (Table S1). Figure 3 E–H displays histograms of the inter-ring torsions angles sampled for the first 10 restricted MD simulations for all molecules. It is evident that the distributions are nearly identical for all biphenyl runs, whereas the distributions vary significantly from run to run for bithiophene. This further demonstrates that the conductance measured in a single bithiophene trace is limited to distinct sets of conformers dependent on the molecule's various geometries as the junction extends.

In summary, we have seen that bithiophene exhibits a broad conductance distribution as compared to biphenyl. By applying a combination of experiment and theory, we have shown that the reduced symmetry of bithiophene leads to a restriction of its inter-ring torsion rotations when confined in a junction. Our work shows the importance of considering the molecular backbone symmetry in designing functional conducting molecular devices.

■ ASSOCIATED CONTENT

📄 Supporting Information

Synthetic, measurement, and computational details. This material is available free of charge via the Internet at <http://pubs.acs.org>.

■ AUTHOR INFORMATION

Corresponding Author

lcampos@columbia.edu; lv2117@columbia.edu

Author Contributions

§E.J.D. and B.C. contributed equally.

Notes

The authors declare no competing financial interest.

■ ACKNOWLEDGMENTS

We thank Dr. Jay Henderson for providing us with a sample of T2. The experimental portion of this work was supported by the NSF (DMR-1206202). The computational work was funded by the Center for Re-Defining Photovoltaic Efficiency through Molecule Scale Control, an EFRC funded by the U.S. Department of Energy, Office of Basic Energy Sciences (de-sc0001085). E.J.D. thanks the HHMI and Dow Chemical Company for International Research Fellowships. T.C.B. was supported by a fellowship from the DOE (SCGF) under Contract No. DE-AC05-06OR23100.

■ REFERENCES

- (1) Aviram, A.; Ratner, M. A. *Chem. Phys. Lett.* **1974**, *29*, 277.
- (2) (a) Xu, B. Q.; Tao, N. J. *Science* **2003**, *301*, 1221. (b) Reichert, J.; Ochs, R.; Beckmann, D.; Weber, H. B.; Mayor, M.; von Lohneysen, H. *Phys. Rev. Lett.* **2002**, *88*, 176804. (c) Zhao, A. D.; Li, Q. X.; Chen, L.; Xiang, H. J.; Wang, W. H.; Pan, S.; Wang, B.; Xiao, X. D.; Yang, J. L.; Hou, J. G.; Zhu, Q. S. *Science* **2005**, *309*, 1542. (d) Venkataraman, L.; Klare, J. E.; Nuckolls, C.; Hybertsen, M. S.; Steigerwald, M. L. *Nature* **2006**, *442*, 904.
- (3) (a) Li, C.; Pobelov, I.; Wandlowski, T.; Bagrets, A.; Arnold, A.; Evers, F. J. *Am. Chem. Soc.* **2008**, *130*, 318. (b) Basch, H.; Cohen, R.; Ratner, M. A. *Nano Lett.* **2005**, *5*, 1668. (c) Quek, S. Y.; Kamenetska, M.; Steigerwald, M. L.; Choi, H. J.; Louie, S. G.; Hybertsen, M. S.; Neaton, J. B.; Venkataraman, L. *Nat. Nano.* **2009**, *4*, 230. (d) Park, Y. S.; Widawsky, J. R.; Kamenetska, M.; Steigerwald, M. L.; Hybertsen, M. S.; Nuckolls, C.; Venkataraman, L. *J. Am. Chem. Soc.* **2009**, *131*, 10820. (e) Mishchenko, A.; Vonlanthen, D.; Meded, V.; Burkle, M.; Li, C.; Pobelov, I. V.; Bagrets, A.; Viljas, J. K.; Pauly, F.; Evers, F.; Mayor, M.; Wandlowski, T. *Nano Lett.* **2010**, *10*, 156.
- (4) (a) Perepichka, I. F.; Perepichka, D. F. *Handbook of thiophene-based materials: applications in organic electronics and photonics*; Wiley: Chichester, U.K., 2009. (b) Sirringhaus, H.; Tessler, N.; Friend, R. H. *Science* **1998**, *280*, 1741. (c) Sirringhaus, H.; Brown, P. J.; Friend, R. H.; Nielsen, M. M.; Bechgaard, K.; Langeveld-Voss, B. M. W.; Spiering, A. J. H.; Janssen, R. A. J.; Meijer, E. W.; Herwig, P.; de Leeuw, D. M. *Nature* **1999**, *401*, 685. (d) Treat, N. D.; Campos, L. M.; Dimitriou, M. D.; Ma, B.; Chabinyc, M. L.; Hawker, C. J. *Adv. Mater.* **2010**, *22*, 4982.
- (5) Park, Y. S.; Whalley, A. C.; Kamenetska, M.; Steigerwald, M. L.; Hybertsen, M. S.; Nuckolls, C.; Venkataraman, L. *J. Am. Chem. Soc.* **2007**, *129*, 15768.
- (6) (a) Milstein, D.; Stille, J. K. *J. Am. Chem. Soc.* **1978**, *100*, 3636. (b) Miyaura, N.; Yamada, K.; Suzuki, A. *Tetrahedron Lett.* **1979**, *20*, 3437.
- (7) Gonzalez, M. T.; Wu, S. M.; Huber, R.; van der Molen, S. J.; Schonenberger, C.; Calame, M. *Nano Lett.* **2006**, *6*, 2238.
- (8) Kamenetska, M.; Koentopp, M.; Whalley, A.; Park, Y. S.; Steigerwald, M.; Nuckolls, C.; Hybertsen, M.; Venkataraman, L. *Phys. Rev. Lett.* **2009**, *102*, 126803.
- (9) DuBay, K. H.; Hall, M. L.; Hughes, T. F.; Wu, C.; Reichman, D. R.; Friesner, R. A. *J. Chem. Theory Comput.* **2012**, *8*, 4556.